1

1 # Titanium oxynitride thin films by the reactive sputtering process with an
2 independent pulsing of O_2 and N_2 gases

3

4 Nicolas Martin*, Jean-Marc Cote, Joseph Gavoille, Jean-Yves Rauch

5 *Institut FEMTO-ST, 15B, Avenue des montboucons, F25030 BESANCON, Cedex, France*

6

7 **Abstract**

8 Titanium oxynitride thin films are deposited by DC reactive magnetron sputtering. A
9 pure titanium target is sputtered in a reactive atmosphere composed of argon, oxygen
10 and nitrogen gases. The oxygen mass flow rate as well as that of the nitrogen gas are
11 both pulsed during the deposition time using an independent and rectangular signal
12 for each reactive gas. A constant pulsing period T = 45 s is applied for both reactive
13 gases and a delay time δ of 34 s between N_2 and O_2 injection times is set for all
14 depositions. Oxygen and nitrogen duty cycles are systematically and independently
15 changed from 0 to 100% of their pulsing period. From real time measurements of the
16 Ti target potential and total sputtering pressure, it is shown that the reactive process
17 alternates between oxidized, nitrided and elemental sputtering modes as a function of
18 the oxygen and nitrogen injection times. The full poisoning of the Ti target surface by
19 oxygen and/or nitrogen can be avoided for some given ranges of O_2 and N_2 duty
20 cycles. Deposition rates of titanium oxynitride films are substantially enhanced and

2 * Corresponding author: nicolas.martin@femto-st.fr; Tel.: +33-363-08-24-31

can be adjusted between that of pure Ti and TiN films with a gradual transition of their electrical conductivity and optical transmittance in the visible range. These results support that titanium oxynitride compounds exhibiting absorbent to transparent behaviors can be precisely sputter-deposited by means of a two reactive gases pulsing process.

Keywords

Titanium oxynitride, reactive sputtering, gas pulsing, target poisoning, duty cycles, enhanced deposition rate.

Introduction

For the last decades, the development of ceramic and semiconducting thin films by vacuum processes has become one of the most challenging tasks for creating functional materials. If binary compounds associating a single metal with a light element such as boron, carbon, nitrogen or oxygen, have been expansively developed by various deposition methods [1-4], the addition of a third element to form ternary compounds still remains pertinent nowadays. These numerous combinations with three different elements may lead to the formation of a homogeneous single phase or even multi-phase disperse system exhibiting various types of designs at the micro- and nanoscale such as nanocomposite structures, solid solutions, or sometimes nanostructured architectures [5-7]. The strategy implemented to grow these ternary thin films strongly depends on the targeted deposited materials. Many studies report on investigations devoted to the fabrication of compounds made of two metals with a metalloid element like oxygen or nitrogen, leading to oxides and nitrides, respectively. [8-12]. Both types of materials can be produced by the sputtering method involving either a ceramic target, or a metallic one and consequently a reactive atmosphere. Since the latter typically exhibits non-linear phenomena of operating parameters (target voltage, deposition rate and so on), they intrinsically restrain some achievable compositions and thus, some physical properties of as-deposited thin films [13]. Some approaches (high pumping speed, feedback control systems …) have been developed to cope with the main drawbacks of the reactive sputtering process. They finally led to get tunable oxide (or nitride) thin films by means of pertinent adjustments of deposition parameters.

11

51 Considering ternary compounds involving a metal combined with two light elements such
52 as oxygen and nitrogen, namely $Me-O_2-N_2$ systems, to prepare oxynitride thin films, the
53 reactive sputtering process becomes even more complex and tricky to control [14-16]. For
54 these thin films, one of the challenging tasks is the high reactivity of oxygen towards the
55 sputtered metal (compared to that of nitrogen), which may limit some reachable compositions
56 and, thus reducing the panel of final properties. A method, namely RGPP – Reactive Gas
57 Pulsing Process, was proposed twenty years ago to easily manage the reactive sputtering
58 process pulsing the most reactive gas, i.e., oxygen, and fabricate oxynitride coatings with
59 tunable oxygen and nitrogen concentrations from pure nitrides to pure oxides [17]. This
60 method was and is still applied to obtain oxides, nitrides and oxynitrides with adjustable
61 metalloid concentrations [18-23]. Resulting properties showed a wide range of behaviors
62 extending from that of nitrides (high hardness, wear resistance …) to oxides (optical
63 transparency, high electrical resistivity …). These behaviors strongly depend on the oxygen
64 and nitrogen amounts in the films [24-28]. However, deposition rates of these oxynitrides still
65 remain much lower than that of metallic rates due to the full poisoning phenomena of the
66 metallic target surface by the reactive gases (alternation of the reactive sputtering process
67 between nitridation and oxidation). As a result, despite the strong potential of RGPP for a
68 possible transfer at an industrial scale, the quite low deposition rate of oxynitride thin films is
69 still a drawback and reaching rates close to that of metal would be a strength of the technique.

70 In this work, we prepare Ti-O-N thin films by reactive sputtering implementing the RGPP
71 technique. The starting point is a pure Ti metallic target sputtered in a reactive atmosphere

14

72 composed of oxygen and nitrogen gases. Compared to previous published studies [23], we
73 report on controlling the reactive sputtering process where both reactive gases are
74 independently and periodically pulsed during the deposition stage. Although many studies
75 report on ceramic thin films based-on oxynitride materials prepared by vacuum processes, it is
76 interesting to focus on the reactive sputtering involving one metallic target and two reactive
77 gases. The motivation of this study is not solely scientific since tunable properties can be
78 reached by playing with simple operating conditions. Due to the well-known instabilities of
79 the reactive process, the latter has to be precisely managed and better understood to get a wide
80 range of thin film behaviors: A challenging task that persists for academic as well as industrial
81 communities. Pulsing both reactive gases is the main motivation of this study since a
82 simultaneous and separate pulsing injection of two reactive gases has never been reported in
83 reactive sputtering processes. In this work, the same O_2 and N_2 pulsing periods are used and a
84 constant delay is applied between the starting points of nitrogen and oxygen injections. Duty
85 cycles related to each gas are systematically investigated from 0 to 100% of each pulsing
86 period of reactive gases. Deposition rate of titanium oxynitride thin films are measured as
87 function of each duty cycle showing rates changing from that of the pure Ti metal to the TiO_2
88 compound. Similarly, the optical transmittance in the visible range (and electrical
89 conductivity) of Ti-O-N thin films show a gradual and well-controlled transition from
90 absorbent (conducting) to transparent (insulating) behaviors. A special emphasis is put on the
91 poisoning state of the Ti target surface assuming real time measurements of the target voltage
92 and total sputtering pressure during the deposition stage. It is shown that alternations between

17

93 2 or 3 sputtering modes (elemental, nitrided, oxidized) can be produced as a function of O_2 and

94 N_2 duty cycles. These alternations are then correlated with evolution of deposition rate,

95 reachable compositions, electrical conductivity and optical transparency of titanium oxynitride

96 thin films.

97

98 **Experimental details**

99 Titanium oxynitride thin films were prepared by DC reactive magnetron sputtering. Details

100 of the deposition system can be found in [19, 23, 26]. Briefly, the sputtering machine was a 60

101 L vacuum reactor evacuated by a turbomolecular pump backed with a mechanical primary

102 pump achieving an ultimate pressure of 5×10^{-6} Pa. A metallic titanium target (51 mm

103 diameter and purity 99.6 at. %) was sputtered in an atmosphere composed of argon, oxygen

104 and nitrogen gases. The substrate was fixed, grounded and located at 65 mm in front of the Ti

105 target. The argon flow rate was kept constant at q_{Ar} = 2.6 sccm and a constant pumping speed

106 S_{Ar} = 13 L s^{-1} was used, leading to an argon partial pressure close to 3.0×10^{-1} Pa. Before any

107 deposition, a pre-sputtering time of 15 min was applied to the Ti target to remove some

108 contamination layers on the target surface and stabilize the process with a Ti target current

109 intensity I_{Ti} = 200 mA corresponding to a current density J_{Ti} = 100 Am^{-2}. For such operating

110 conditions, the Ti target potential in pure argon sputtering atmosphere reached U_{Ti} = 305 V.

111 Afterwards, nitrogen and/or oxygen gases were introduced using independent pulsing signals

112 for each reactive gas. To this aim, a homemade computer-controlled system, namely, the

113 reactive gas pulsing process (RGPP) was developed to manage accurately reactive gas mass

20

114 flow rate *vs.* time [23]. In this paper, both gases were separately injected following a
115 rectangular pulsing signal (Fig. 1).

116 Except injection times of each reactive gas (i.e., t^{O2}_{ON} and t^{N2}_{ON} related to O_2 and N_2 gases,
117 respectively) all the other pulsing parameters described in Fig. 1 were kept constant. Minimum
118 O_2 and N_2 flow rates (q^{O2}_{min} and q^{N2}_{min}, respectively) were both fixed at 0 sccm in order to
119 completely stop the oxygen and nitrogen injections during the corresponding t^{O2}_{OFF} and t^{N2}_{OFF}
120 times, respectively. For maximum O_2 and N_2 flow rates, q^{O2}_{Max} = 2.0 sccm and q^{N2}_{Max} = 0.8
121 sccm. These maximum values correspond to the amount of reactive gas (O_2 or N_2) required to
122 fully poison (oxidized or nitrided, respectively) the Ti target when the reactive gas is
123 constantly and solely injected in the process. In order to better control the reactive process, the
124 pulsing period of both gases were set to $T_{O2} = T_{N2} = T$ = 45 s. This choice is based-on previous
125 investigations showing that the reactive sputtering process involving one Ti metallic target
126 sputtered in a reactive atmosphere (especially O_2), can alternate between poisoned and
127 elemental modes by playing with the time of reactive gas injection (i.e., t_{ON} time) [29].

23

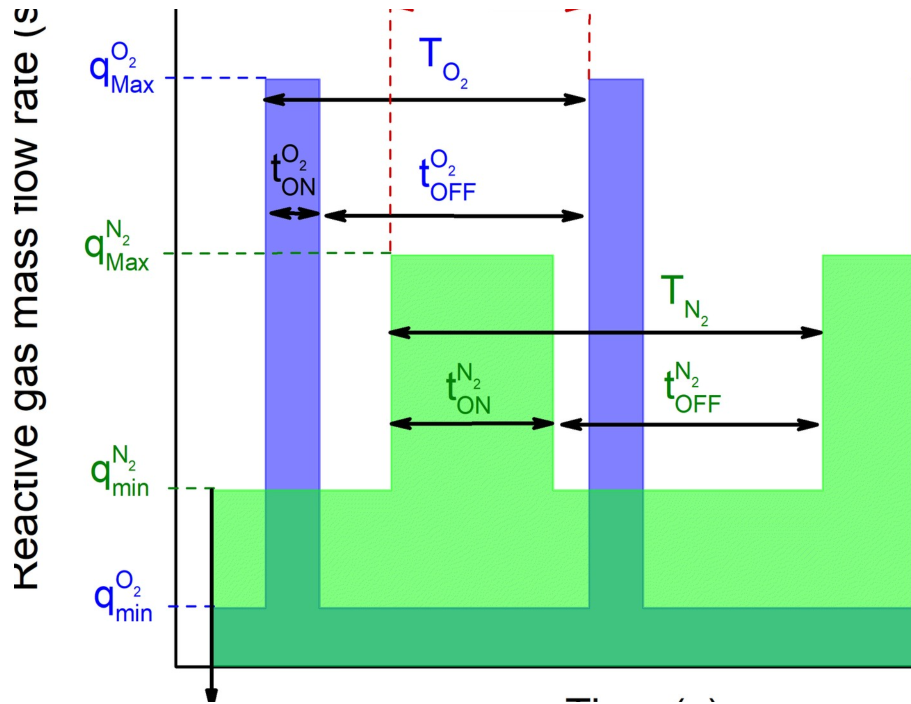

128

129 *Fig. 1. Oxygen and nitrogen mass flow rates as a function of the time implemented during the*
130 *sputter-deposition of Ti-O-N thin films. A rectangular signal is used for both reactive gases,*
131 *which are independently and periodically pulsed during the deposition. All pulsing*
132 *parameters can be tuned for each gas.* T_{O2} *= pulsing period of* O_2 *(s),* T_{N2} *= pulsing period of*
133 O_2 *(s),* δ *= delay time between the starting point of* N_2 *and* O_2 *pulsing (s),* $q^{O2}{}_{min}$ *= minimum* O_2
134 *flow rate (sccm),* $q^{N2}{}_{min}$ *= minimum* N_2 *flow rate (sccm),* $q^{O2}{}_{Max}$ *= maximum* O_2 *flow rate*
135 *(sccm),* $q^{N2}{}_{Max}$ *= maximum* N_2 *flow rate (sccm),* $t^{O2}{}_{ON}$ *= time of* O_2 *injection at* $q^{O2}{}_{Max}$ *(s),* $t^{O2}{}_{OFF}$
136 *= time of* O_2 *injection at* $q^{O2}{}_{min}$ *(s),* $t^{N2}{}_{ON}$ *= time of* N_2 *injection at* $q^{N2}{}_{Max}$ *(s),* $t^{N2}{}_{OFF}$ *= time of* N_2
137 *injection at* $q^{N2}{}_{min}$ *(s).*

138

139 Last but not least concerns the delay time, namely δ, defined as the time between the
140 starting point of N_2 and O_2 pulsing. This δ parameter was chosen at $\delta = 34$ s (i.e., 75% of T).
141 This allows an adjustment of the kinetics of the reactive process by playing only with times of
142 each reactive gas injection, especially so as to restore the process to the elemental mode during
143 the t^{O2}_{OFF} time, and before the injection of N_2 (i.e., before the starting point of the t^{N2}_{ON} time).
144 Since the main purpose of this study is focused on the deposition of tunable titanium
145 oxynitride thin films, t^{O2}_{ON} and t^{N2}_{ON} times were systematically changed from 0 to 100 % of the
146 pulsing period T. In other words, the duty cycles of O_2 and N_2 gases defined as $\alpha_{O2} = t^{O2}_{ON}/T$
147 and $\alpha_{N2} = t^{N2}_{ON}/T$ were gradually modified (α_{O2} and α_{N2} are in between 0-1). However, and for
148 convenience, they are stated in percentage of the pulsing period T. For all depositions, real
149 time measurements of the Ti target voltage and total sputtering pressure were recorded. These
150 parameters give information about the state of poisoning of the Ti target surface.

151 All films were deposited on glass (microscope slides $25\times10\times1$ mm^3) and (100) Si
152 substrates ($25\times10\times0.5$ mm^3). The latter were ultrasonically cleaned with acetone and alcohol
153 for 15 minutes before each run. During deposition, substrates were grounded and no external
154 heating was used. The deposition time was adjusted in order to produce films with the same
155 thickness (close to 300 nm and measured with a Bruker Dektak profilometer). The chemical
156 composition of films prepared on (100) Si was determined by electron probe microanalysis
157 (EPMA) with the wavelength dispersion method. Optical transmittance spectra of films
158 prepared on glass was measured in the visible range (from 200 to 900 nm with a scan speed of
159 1 nm s^{-1}) with a Lambda 20 UV-Vis Perkin-Elmer spectrophotometer. This optical

160 characteristic is particularly interesting since it informs about transparency of the films for
161 optical and decorative applications (an average optical transmittance was calculated at 633 nm
162 since this is a reference wavelength of Helium-Neon laser commonly used in optics). The DC
163 electrical resistivity was measured at room temperature (home made system) for films
164 deposited on glass using the four probe method with the van der Pauw configuration.
165

166 **Results and Discussion**

167 The deposition rate of Ti-O-N films was measured as function of the oxygen duty cycle α_{O2}
168 and for various nitrogen duty cycles α_{N2} (Fig. 2). Without pulsing the nitrogen gas and based
169 on previous results [29], a continuous evolution of the deposition rate *vs.* oxygen duty cycle
170 α_{O2} is clearly measured. The typical feature associated to the conventional reactive sputtering
171 process exhibiting a sudden drop of the deposition rate as a function of the reactive gas flow
172 rate is not produced by RGPP. The deposition rate is nearly constant up to α_{O2} = 33% of T_{O2}
173 and close that of TiN rate (around 260 nm h^{-1}). For O_2 duty cycles higher than 70% of T_{O2}, the
174 rate regularly decreases and tends to be stable at 120 nm h^{-1}. The lowest rate is obtained for
175 TiO_2 thin films prepared with a constant supply of the oxygen gas. As RGPP is applied to the
176 deposition of titanium oxynitride thin films, instabilities of the reactive sputtering process can
177 be avoided and the sudden change of many experimental parameters for some given nitrogen
178 and oxygen flow rates, particularly the abrupt drop of the deposition rate due to poisoning of
179 the target surface by oxygen, is circumvented. A smooth evolution is obtained instead of a

180 non-linear phenomenon as the oxygen duty cycle increases, especially for oxygen duty cycles

181 included between 33 and 70% of T_{O2}.

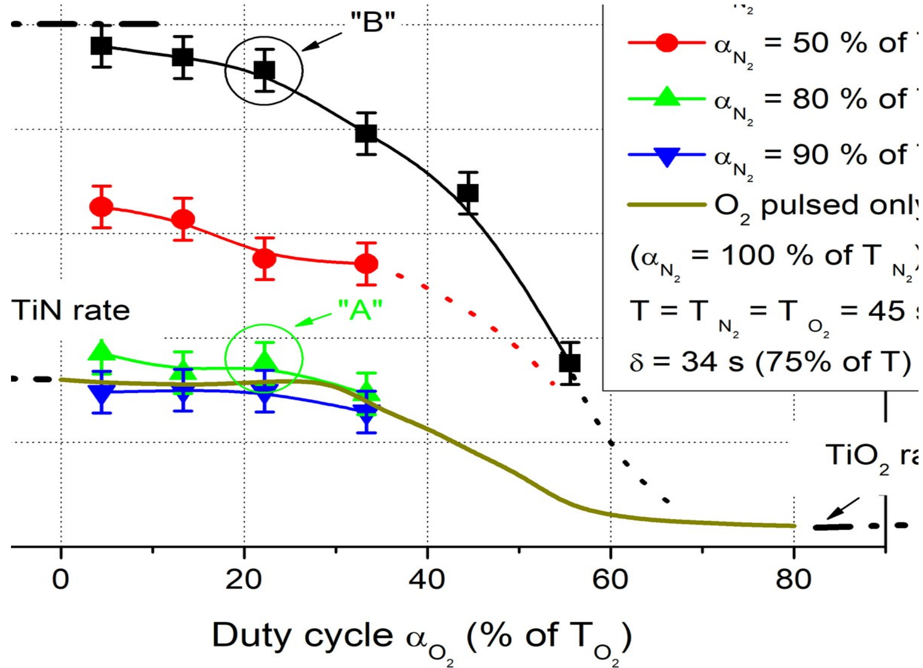

182

183 *Fig. 2. Ti-O-N deposition rate as a function of the oxygen duty cycle α_{O2} and for various*

184 *nitrogen duty cycles α_{N2}. Both reactive gases are pulsed with the same period, i.e., $T = T_{O2} =$*

185 *T_{N2} = 45 s, and the delay time δ = 34 s (i.e., 75% of the pulsing period T). Ti, TiN and TiO_2*

186 *deposition rates are also specified in pure argon atmosphere, when nitrogen and oxygen are*

187 *constantly injected at q_{N2Max} and q_{O2Max}, respectively. Operating conditions noted "A" and "B"*

188 *will be discussed from real time measurements of Ti target potential and total sputtering*

189 *pressure.*

190

35

191 Pulsing the nitrogen gas at the same time as the oxygen gas does not lead to significant
192 changes of the deposition rate *vs.* oxygen duty cycle α_{O2} for nitrogen duty cycle α_{N2} in-between
193 80-100% of the N_2 pulsing period. The rate remains nearly constant up to α_{O2} = 33% of T_{O2}
194 with values very close to that of the reactive process implementing the single O_2 pulsing.
195 Afterwards (not shown in Fig. 2 for clarity), a similar smooth drop of the rate is measured as
196 the oxygen duty cycle changes from 33 to 70% of the oxygen pulsing period. For α_{O2} < 33% of
197 T_{O2}, despite short t^{O2}_{ON} times (in the order of a few seconds) and due to the high reactivity of
198 titanium towards oxygen, the process avalanches rapidly in the oxidized sputtering mode.
199 During the t^{O2}_{OFF} time, it is long enough to restore the process in the nitrided sputtering mode.
200 As a result, the process alternates between nitrided and oxidized sputtering modes assuming
201 oxygen duty cycles lower than 70% of T_{O2}. For higher α_{O2}, the t^{O2}_{OFF} time becomes too short
202 and the process is completed trapped in the oxidized sputtering mode.
203 On the other hand, nitrogen duty cycles lower than 80% of the pulsing period give rise to a
204 relevant enhancement of the deposition rate. For α_{N2} = 50% of T_{N2} and considering the lowest
205 oxygen duty cycles (e.g., α_{O2} < 20% of T_{O2}), it is worth noting that the deposition rate is
206 strongly boosted and exceeds 400 nm h^{-1}. This enhanced deposition rate is even greater for α_{N2}
207 = 25% of T_{N2} since it tends to be close to the Ti metallic rate, which can be assumed as a
208 reference in a deposition system and for some given sputtering conditions in pure argon
209 atmosphere (i.e., close to 600 nm h^{-1}). For such operating conditions, both t^{O2}_{ON} and t^{N2}_{ON} times
210 are shorter than ten seconds and both t^{O2}_{OFF} and t^{N2}_{OFF} times are long enough to restore the
211 process in the elemental mode, mainly (it will be more discussed later from Ti target potential

38

212 *vs.* time measurements). Since the sputtering yield of titanium oxide is lower than that of
213 titanium nitride, which is itself lower than that of pure titanium [30], one can expect the
214 highest deposition rates when the process runs predominantly in the elemental sputtering
215 mode. For the shortest nitrogen duty cycles, it is also interesting remarking that the deposition
216 rate is very sensitive to the oxygen injection, as shown for α_{N2} = 25% of T_{N2} in Fig. 2. The
217 small decrease of rate measured up to α_{O2} = 20% of T_{O2} becomes more marked in between 25-
218 60% of T_{O2} with a halved rate, and finally with a trend to achieve TiO_2- like rate. The
219 oxidation of the Ti target surface prevails even for the very short nitrogen injection times,
220 where the process is trapped in the oxidized sputtering mode.

221 Ti-O-N films sputter-deposited on glass substrates also exhibit optical transmittance in the
222 visible range (at 633nm), which strongly depends on oxygen and nitrogen pulsing conditions
223 (Fig. 3a). With a constant nitrogen flow rate and pulsing only the oxygen gas, absorbent Ti-O-
224 N films are produced for oxygen duty cycles lower than a few % of T_{O2}. Films become
225 gradually transparent for α_{O2} > 10% of T_{O2} and then completely interferential with a TiO_2-like
226 behaviors for α_{O2} > 40% of T_{O2} where a further increase of oxygen duty cycle does not change
227 the optical transparency with an average of 80% of transmittance at 633 nm. As a result, the
228 most interesting range of oxygen duty cycles leading to relevant changes of the Ti-O-N optical
229 properties is in-between 10-40% of T_{O2}. Assuming the evolution of deposition rate *vs.* α_{O2}
230 earlier discussed from results in Fig. 2, this range is located before the significant drop of the
231 rate.

39
40

41

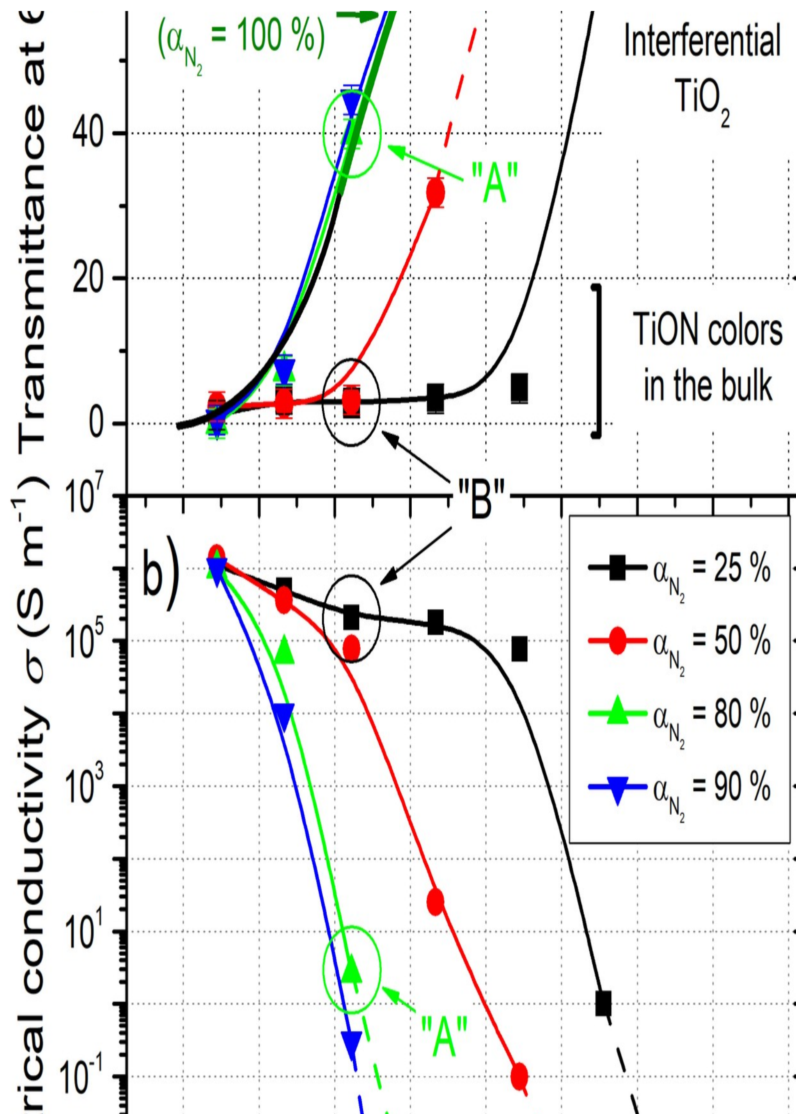

232

233 *Fig. 3. a) Optical transmittance at 633 nm and b) DC electrical conductivity at room*
234 *temperature vs. oxygen duty cycle of Ti-O-N thin films 400 nm thick deposited on glass*
235 *substrates for various nitrogen duty cycles. A smooth transition can be obtained from*
236 *absorbent Ti-O-N films colored in the bulk, to interferential TiO_2-like compounds as a*
237 *function of oxygen and nitrogen duty cycles. It also correlates with a significant change of the*

44

238 *electrical properties from conducting to semi-conducting and finally insulating behaviors.*
239 *Optical and electrical properties of films prepared following "A" and "B" points (as reported*
240 *in Fig. 2) are also given.*

241

242 As previously noticed for deposition rate *vs.* α_{O2}, pulsing the nitrogen gas does not
243 necessarily induce relevant changes in the optical transmittance of the films. For nitrogen duty
244 cycles higher than 80% of T_{N2}, the gradual and smooth change of optical transmittance as a
245 function of α_{O2} is obtained for the same range of oxygen duty cycles (i.e., in-between 10-40%
246 of T_{O2}).

247 The regular absorbent-to-transparent transition is clearly shifted to higher oxygen duty
248 cycles for Ti-O-N thin films prepared with nitrogen duty cycles lower than 50% of T_{N2}. It is
249 even more noticeable for α_{N2} = 25% of T_{N2} since films prepared with α_{O2} = 45% of T_{O2} still
250 exhibit an optical transmittance at 633 nm lower than a few %. This range of oxygen duty
251 cycles correlates with the highest deposition rates (close to the Ti metallic rate) and before the
252 substantial drop of the rate corresponding to a predominant poisoning of the Ti target surface
253 by the oxygen gas, as reported in Fig. 2. These results also support that adjusting
254 simultaneously and independently both reactive gas duty cycles allows an extension of the
255 reactive sputtering conditions suitable to produce absorbent Ti-O-N thin films with colors in
256 the bulk.

257 Similarly, electrical properties of the films strongly depend on oxygen and nitrogen duty
258 cycles as shown in Fig. 3b. For any nitrogen duty cycle, films systematically become more

259 resistive as the oxygen duty cycle rises. For α_{N2} = 25% of T_{N2}, and up to α_{O2} = 44% of T_{O2},
260 conductivity σ is higher than 10^5 S m^{-1} with a metallic-like behavior. A further increase of α_{O2}
261 leads to a sudden drop of σ (more than 5 orders of magnitude) and films become too much
262 resistive to be measured with our four probe system. This σ *vs.* α_{O2} feature is even more
263 noticeable when α_{N2} increases and tends to a constant nitrogen supply. This drop of
264 conductivity is shifted to the shortest ranges of α_{O2} since more oxygen is introduced in the
265 process and thus in the films. It is worth noting that optical transmittance and electrical
266 conductivity exhibit a reverse evolution as a function of α_{O2} and α_{N2}. , which agree with
267 previous studies reported for other metallic oxynitrides [22-29] and mainly assigned to an
268 oxygen-enrichment of the films.

269 The real time measurement of the Ti target potential U_{Ti} and total sputtering pressure $P_{Sput.}$
270 *vs.* time is a simple and valuable approach to follow instabilities of the reactive sputtering
271 process [17]. This potential *vs.* time recording is typical of the poisoning state of the target
272 surface by the reactive gas and characterizes the kinetics of poisoning. In this study, these
273 measurements have been performed for operating conditions corresponding to the deposition
274 of semi-transparent and absorbent Ti-O-N films, as indicated by point “A” and “B” in Fig. 2
275 (and 3), respectively. Figure 4a shows some typical measurements of U_{Ti} and $P_{Sput.}$ *vs.* time for
276 films prepared with α_{O2} = 22% of T_{O2} and α_{N2} = 80% of T_{N2} (semi-transparent films – point
277 “A”).

50

278

279 *Fig. 4. a) Real time measurements of Ti target potential and total sputtering pressure*
280 *recorded during Ti-O-N film deposition setting* α_{N2} *= 80% of* T_{N2} *and* α_{O2} *= 22%* T_{O2}*. Pulsing*
281 *period* $T = T_{O2} = T_{N2} = 45$ *s and delay time* $\delta = 34$ *s. These operating conditions correspond*
282 *to the preparation of semi-absorbent films (point "A" in Fig. 2 and 3). b) Real mass flow*
283 *rates vs. time of oxygen and nitrogen gases are also specified and can be easily compared to*
284 *response times of potential and pressure.*

285

286 Real mass flow rates of both reactive gases are also given in order to show how times of
287 injection and nature of the reactive gas influence the process. They also illustrate that the
288 response time of mass flowmeters are very short (less than 1 second) to introduce and/or to

53

289 stop reactive gas injections despite of unsuitable overshoots and adjustments of setpoints at the
290 beginning of injections.

291 For these pulsing conditions, it is first important noticing that the sputtering process is
292 always in reactive mode although the interval starting at the end of t^{O2}_{ON} and finishing at the
293 beginning of t^{N2}_{ON} produces a short gap (for 1 to 2 s as shown in Fig. 4b) without any reactive
294 gas injection. This leads to a total sputtering pressure of 4.3×10^{-1} Pa corresponding to a
295 nitrided sputtering mode. The Ti target potential is also influenced by O_2 and N_2 pulsing (Fig.
296 4a). When oxygen is introduced (beginning of the t^{O2}_{ON} time), U_{Ti} abruptly rises from 344 V
297 (nitrided mode) to 415 V in a few hundred milliseconds, then drops down to 375 V till the end
298 of the oxygen injection. This is assigned to the high reactivity of oxygen towards titanium,
299 which is enhanced when the reactive process runs in the nitrided mode [16]. In addition,
300 diffusion of reactive ionic species, chemisorption, knock-in [31] as well as implantation in the
301 Ti target [32, 33] all induce surface modifications. The Ti target behavior is then strongly
302 affected by the formation of some complex compounds (certainly a mixture of titanium
303 oxides, nitrides and oxynitrides a few nm thick) reducing the sputtering yield and inducing the
304 typical hysteresis phenomena of the reactive sputtering process.

305 In the same way, the total sputtering pressure increases and stabilizes around 5.3×10^{-1} Pa,
306 corresponding to the oxidized mode of the reactive sputtering process. Stopping the oxygen
307 injection and starting the nitrogen one gives rise to a second sharp peak of the Ti target
308 potential, again at about 415 V. It is closely linked to the return of the process in the nitrided
309 mode with a speeder implementation since the second peak is sharper than the first one. As a

56

310 result, the reactive sputtering process is not at steady state conditions but periodically
311 alternates between the nitrided and oxidized mode. For such operating parameters, it
312 predominates in the nitrided mode since U_{Ti} still decreases at the end of the t^{O2}_{ON} time (despite
313 a nearly constant pressure), whereas potential tends to become constant when nitrogen is
314 solely introduced (end of the t^{N2}_{ON} time).

315 Keeping the same oxygen injection time (i.e., α_{O2} = 22% of T_{O2}) and reducing that of
316 nitrogen to α_{N2} = 25% of T_{N2} extends the time of sputtering without reactive gas injection.
317 Applying these experimental parameters also allow supplying one reactive gas at a time (Fig.
318 5).

319

59

320 *Fig. 5. a) Real time measurements of Ti target potential and total sputtering pressure*
321 *recorded during Ti-O-N film deposition setting α_{N2} = 25% of T_{N2} and α_{O2} = 22% T_{O2}. Pulsing*
322 *period T = T_{O2} = T_{N2} = 45 s and delay time δ = 34 s. These operating conditions correspond*
323 *to the preparation of absorbent films (point "B" in Fig. 2 and 3). b) Real mass flow rates vs.*
324 *time of oxygen and nitrogen gases are also specified and can be easily compared to response*
325 *times of potential and pressure.*

326

327 Before injecting reactive gases, U_{Ti} is the lowest. It reaches 305 V and the total sputtering
328 pressure is 3.7×10^{-1} Pa at the end of the t^{O2}_{OFF} time. The process is in the elemental sputtering
329 mode. Pulsing O_2 at first produces again a sudden increase of the Ti target potential to more
330 than 405 V with a sharp peak at the beginning of the t^{O2}_{ON} time. The total sputtering pressure
331 continues to grow until the end of the t^{O2}_{ON} time and a longer O_2 injection would avalanche the
332 process in the oxidized mode only. Stopping O_2 injection does not completely stabilize U_{Ti} and
333 introducing N_2 leads to the same peak of the target potential, but narrower. Pressure tends to
334 4.3×10^{-1} Pa during the t^{N2}_{ON} time, which means that the process is in the nitrided mode.
335 Similarly, when the two reactive gases are stopped, potential as well as pressure both reduce
336 and come back to values obtained before pulsing O_2 (305 V and 3.7×10^{-1} Pa, respectively) ,
337 and so the process is restored to the elemental mode. These results show that reducing the time
338 of O_2 injection does not completely trap the reactive sputtering process in the poisoned mode
339 by O_2 or N_2. Therefore, reactive gas duty cycles are two key parameters to alternate the
340 process between 3 modes: oxidized, nitrided and elemental.

62

341 Both duty cycles have been systematically changed from 0 to 100% of the same pulsing
342 period $T = T_{O2} = T_{N2} = 45$ s, and real time measurements of potential and pressure have also
343 been recorded. Some examples are given in Fig. 6 in order to illustrate the tunability of the
344 reactive sputtering process between the different modes by changing only α_{O2} and α_{N2}.

345 For low duty cycles like $\alpha_{O2} = 4\%$ of T_{O2} and $\alpha_{N2} = 25\%$ of T_{N2}, t^{O2}_{OFF} and t^{O2}_{OFF} times are
346 both long enough to restore the process in the elemental mode since the Ti target potential is
347 constant and reaches 305 V before introducing O_2 or N_2 with a total sputtering pressure of
348 3.7×10^{-1} Pa. The very short introduction of oxygen gives rise to small peaks of U_{Ti} without a
349 noticeable change of pressure. On the other hand, the pulsing time of nitrogen is longer for α_{N2}
350 = 25 and 50% of T_{N2} to set the process in the nitrided mode with U_{Ti} stabilizing at 332 V and
351 pressure tending to 4.3×10^{-1} Pa. These pulsing conditions show that the oxidized state is not
352 achieved and the process mainly alternates between nitrided and elemental modes. A further
353 increase of t^{N2}_{ON} time ($\alpha_{N2} = 80\%$ of T_{N2}) allows a more oxidized state (U_{Ti} overpasses 405 V
354 with a corresponding peak of pressure), but reduces the time kept in the elemental mode. The
355 nitrided mode predominates for $\alpha_{O2} = 4\%$ of T_{O2} and $\alpha_{N2} = 80\%$ of T_{N2}, and these operating
356 conditions set the process between the 3 modes (increasing more α_{N2} traps the process in the
357 nitrided mode).

358 This alternation between the 3 modes is even more obtained with $\alpha_{O2} = 22\%$ of T_{O2} and α_{N2}
359 = 25% of T_{N2}, or even $\alpha_{O2} = 33\%$ of T_{O2} and $\alpha_{N2} = 50\%$ of T_{N2}, as shown in Fig. 6. Assuming a
360 single pulsing period (for 45 s), the shape of U_{Ti} and pressure *vs.* time are very similar for
361 these sputtering conditions. Two sharp peaks of the Ti target potential are observed due to

63

64

65

362 oxidized then nitrided mode. They are followed by a shoulder and a trend to achieve the
363 lowest and stable value of 305 V assigned to the return to the elemental mode. Extending both
364 duty cycles leads to an overlapping of O_2 and N_2 pulsing signals where the oxidized state
365 prevails over the nitrided one since oxygen is more reactive towards titanium. It particularly
366 reduces the time for restoring the process in the elemental mode and an alternation between
367 oxidized and nitrided modes is only possible. These conditions are particularly established for
368 α_{O2} = 22% of T_{O2} and α_{N2} = 80% of T_{N2} (or α_{O2} = 33% of T_{O2} and α_{N2} = 80% of T_{N2}, as
369 illustrated in Fig. 6) where the Ti target potential never comes back to 305 V and the total
370 sputtering pressure cannot go below 4.3×10^{-1} Pa.

66
67

68

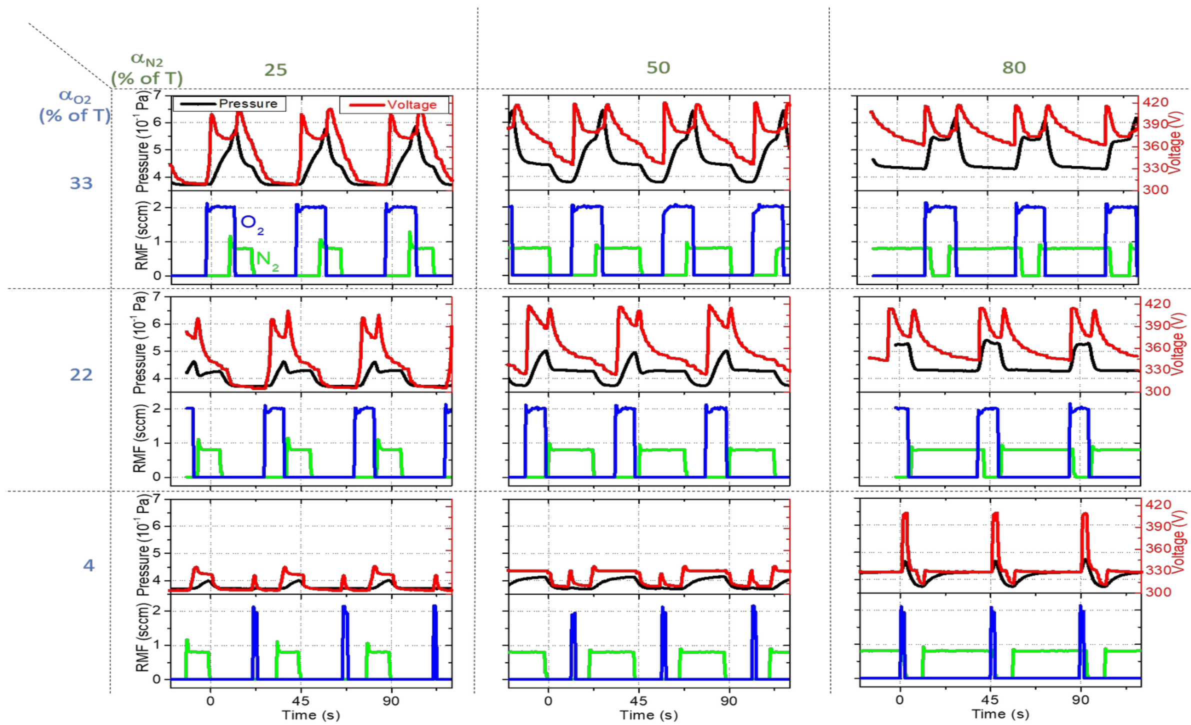

371

372 *Fig. 6. a) Real time measurements of Ti target potential and total sputtering pressure*

373 *recorded during Ti-O-N film deposition for various α_{N2} and α_{O2} duty cycles. Pulsing period T*

374 *= T_{O2} = T_{N2} = 45 s and delay time δ = 34 s. Real mass flow rates (RMF) vs. time for oxygen*

375 *and nitrogen gases are also shown.*

376

377 Using all real time measurements of Ti target potential and total sputtering pressure *vs.* time

378 systematically recorded for duty cycles varying from 0 to 100% of T, a qualitative 2D diagram

379 is built. It defines boundaries of the reactive sputtering process alternations between 1, 2 or 3

71

380 modes taking into account O_2 and N_2 duty cycles only (Fig. 7). This kind of 2D diagram
381 showing the state of the reactive sputtering process *vs.* reactive gas supply has ever been
382 suggested and built for the deposition of titanium oxynitride thin films by conventional
383 method [16] (i.e., constant supply of O_2 and N_2). However, it has never been implemented for
384 two reactive gases independently pulsed by RGPP. This diagram represents how the different
385 modes of the reactive sputtering process can be favored as a function of O_2 and N_2 pulsing
386 injections, and so one can deduce the type of titanium oxynitride thin films that can be sputter-
387 deposited. For operating conditions used in this study, the process is mainly in the elemental
388 sputtering mode for the lowest O_2 and N_2 duty cycles (grey zone, namely Ti in Fig. 7) since t_{ON}
389 times are too short to completely poison the Ti target surface by oxygen and/or nitrogen. This
390 correlates with the highest deposition rates of Ti-O-N films (close to that of Ti) previously
391 reported in Fig. 2.

72
73

74

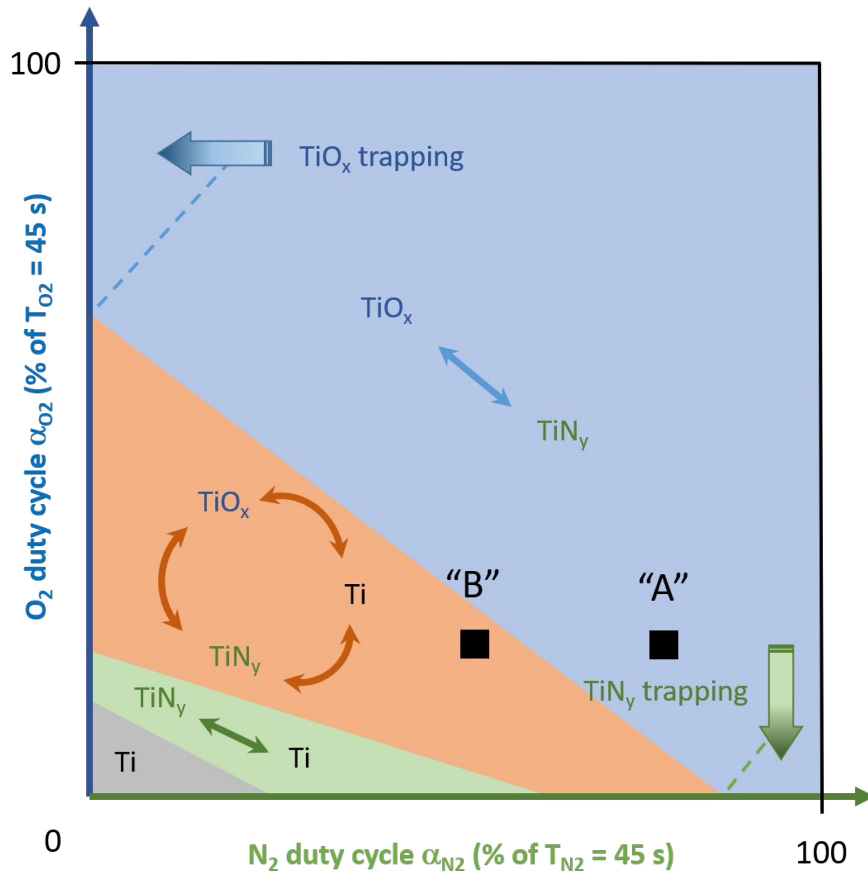

392

393 *Fig. 7. 2D qualitative diagram for the reactive sputtering of Ti-O-N thin films by RGPP with*
394 *an independent pulsing of oxygen and nitrogen reactive gases. Occurrence of different*
395 *reactive sputtering modes (elemental, nitrided or oxidized) are defined as a function of* O_2 *and*
396 N_2 *duty cycles. A periodic alternation of the process between 2 or 3 modes can be tuned by*
397 *means of an accurate control of both duty cycles. Points "A" and "B" are also indicated from*
398 *operating conditions defined in Fig. 2.*

399

77

400 Increasing duty cycles (especially for N_2) leads to an alternation of the process between
401 elemental and nitrided modes (green zone, $TiN_y \leftrightarrow Ti$ in Fig. 7). Injecting for a longer time
402 one of the reactive gas or both gives rise to a periodic alternation of the process between the 3
403 modes: elemental, nitrided and oxidized ones (orange zone, $TiO_x \leftrightarrow TiN_y \leftrightarrow Ti$ in Fig. 7). This
404 zone is connected to the drop of the deposition rate *vs.* α_{O2} formerly reported in Fig. 2, but also
405 to the gradual transition from absorbent (conducting) to transparent (insulating) Ti-O-N films
406 measured from optical transmittance in Fig. 3. For the highest duty cycles, the process is then
407 fully in compound sputtering mode and may be pulsed between oxidized and nitrided modes
408 (blue zone, $TiO_x \leftrightarrow TiN_y$ in Fig. 7). It corresponds to the deposition of interferential thin films
409 produced with the lowest deposition rates. It is worth noting that the process can be trapped
410 either in nitrided, or oxidized sputtering mode when duty cycle values are opposite from each
411 other, i.e., α_{O2} tending to 100% of T_{O2} (and inversely α_{N2} tending to 0% of T_{N2}) and *vice versa*.
412 Although sizes and boundaries between zones still remain qualitative and are not accurately
413 defined, they allow the occurrence of sputtering regimes and the range of transitions between
414 1, 2 or 3 modes. As similarly reported for instabilities of the reactive sputtering process
415 involving one metallic target with one reactive gas (basic system by conventional reactive
416 sputtering), boundaries of the different zones depend on the reactivity of the metal towards
417 oxygen and nitrogen species, geometry and dimensions of the sputtering chamber,
418 experimental parameters such as pumping speed, target current and so on. As a result, playing
419 with parameters influencing sizes and features of instabilities may favor a zone than another
420 one and then a given sputtering mode.

80

421 All films have been deposited on substrates at room temperature, i.e., without external
422 heating. For such operating conditions and when a reactive gas like O_2 or N_2 is pulsed, or
423 when N_2 is constantly supplied whereas O_2 is periodically introduced, it was previously shown
424 that films adopt an amorphous structure, except for the lowest duty cycles (a few % of the
425 pulsing period P) where films are poorly crystalline and show small diffracted signals
426 corresponding to the hexagonal structure of Ti compound [20, 23]. Similar results have been
427 obtained in this study with a systematic amorphization of titanium oxynitride thin films
428 increasing both duty cycles. As a result, the film properties mainly depend on their chemical
429 composition, the latter being largely influenced by the reactive gas injection (pulsed or not)
430 and by duty cycles, as shown in Fig. 8.

81
82

83

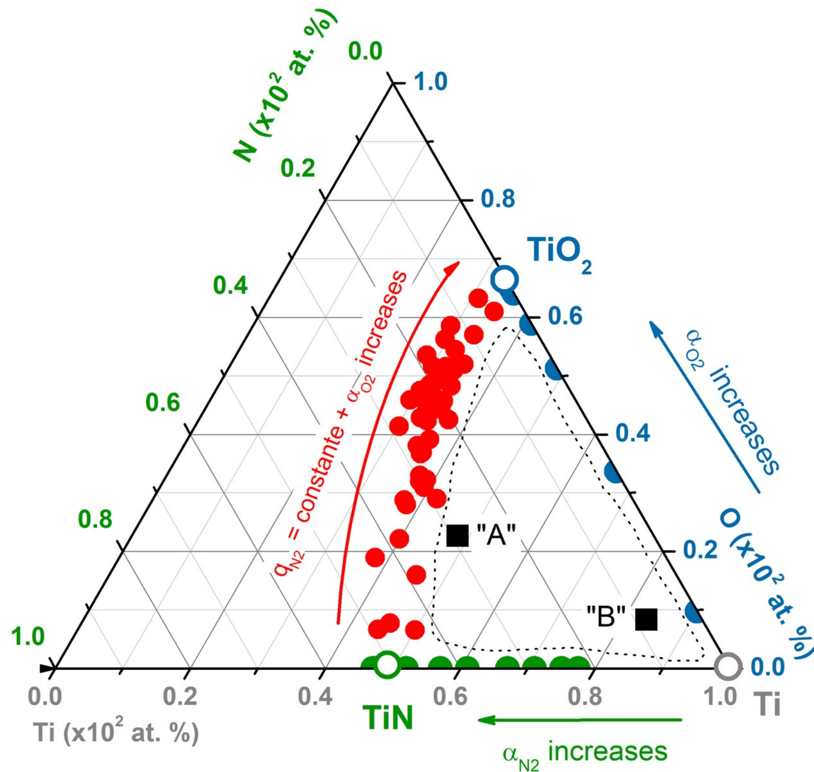

431

432 *Fig. 8. Ternary phase diagram illustrating the range of chemical compositions which can be*
433 *achieved in titanium oxynitride thin films sputter-deposited pulsing only* O_2 *gas and keeping*
434 *constant* N_2 *flow rate(red circles from [34]), or pulsing independently both reactive gases*
435 *(triangular region defined by the dotted black line with points "A" and "B" - black squares -*
436 *as defined previously from Fig. 2). Compositions of* TiN_y *and* TiO_x *films produced by RGPP*
437 *introducing and pulsing only one reactive gas (*N_2 *and* O_2*, respectively) are also indicated*
438 *(green and blue circles, respectively).*

439

86

440 This ternary diagram shows the range of oxide and nitride thin films which can be produced
441 by supplying and pulsing only one reactive gas with a precise adjustment of the corresponding
442 duty cycle (i.e., α_{O2} and α_{N2}, respectively) . For oxynitride compounds, pulsing O_2 while N_2 is
443 constantly injected in the process gives rise to a gradual variation of both metalloid
444 concentrations (red circles in Fig. 8). However, the region delimited by the triangular-like
445 shape plotted with the black dotted line cannot be reached pulsing only the oxygen gas
446 keeping a constant nitrogen mass flow rate. Such a drawback is completely solved with an
447 independent pulsing of O_2 and N_2. Playing simultaneously with α_{O2} and α_{N2} clearly extends the
448 reachable titanium oxynitride thin films. Points "A" and "B" corresponding to operating
449 conditions defined in Fig. 2 are located in this region. There are typical examples of extended
450 compositions obtained by means of this two reactive gas pulsing approach.
451
452
453 **Conclusions**
454 The reactive gas pulsing process, namely RGPP, is developed to produce titanium
455 oxynitride thin films. A pure Ti metallic target is sputtered in a reactive atmosphere of Ar, O_2
456 and N_2 gases. Both reactive gases are simultaneously and independently pulsed with a
457 rectangular signal during the deposition of Ti-O-N films. A constant pulsing period T = 45 s is
458 used for O_2 and N_2 gases with a delay time δ = 34 s between the starting injection of each
459 reactive gas. O_2 and N_2 duty cycles (α_{O2} and α_{N2}, respectively) are systematically changed from
460 0 to 100% of T.

89

461 For N_2 duty cycles higher than α_{N2} =80% of T, deposition rate *vs.* O_2 duty cycle exhibits a
462 similar evolution as those obtained pulsing only the oxygen gas while the nitrogen gas is
463 constantly introduced. No sudden drop of the deposition rate is measured with the oxygen
464 pulsing, but a regular reduction from that of TiN and TiO_2 as α_{O2} increases, which corresponds
465 to a smooth absorbent-to-transparent transition of the optical transmittance of the films in the
466 visible region and a continuous evolution of their electrical properties from conducting to
467 insulating materials. From real time measurements of the Ti target potential and total
468 sputtering pressure, it is shown these experimental conditions alternate the reactive sputtering
469 process between nitrided and oxidized sputtering modes.

470 Operating with N_2 duty cycles lower than α_{N2} = 80% of T leads to a substantial increase of
471 the deposition rate for any α_{O2} with values approaching to that of the pure Ti compound. These
472 lower N_2 duty cycles also allow extending the working range of α_{O2} suitable to tune electrical
473 behaviors and optical transmittance of the Ti-O-N films from absorbent (color in the bulk) to
474 interferential. Analyses of Ti target potential and total sputtering pressure *vs.* time show that
475 the process periodically changes between 3 modes: elemental, nitrided and oxidized.

476 A 2D qualitative diagram based-on O_2 and N_2 duty cycles as the 2 key parameters is finally
477 proposed. Even though accuracy of sizes and boundaries delimited between zones still remain
478 questionable, occurrence of different reactive sputtering regimes is defined with transitions
479 between periodic alternations of the process according to 2 or 3 modes. Such a diagram clearly
480 illustrates that these alternations between elemental, nitrided or oxidized sputtering conditions
481 can be produced as a function of O_2 and N_2 duty cycles. They also well correlate with variation

90
91

92

482 of deposition rate, optical transparency and extended compositions of titanium oxynitride thin
483 films. As a result, it clearly proves that and independent pulsing injection of O_2 and N_2 by the
484 RGPP technique is a valuable way to control the reactive sputtering process, and to prepare a
485 wide panel of Ti-O-N thin films with tunable properties.

486

487 **Acknowledgments**

488 This work has been supported by the Région Bourgogne Franche-Comté. This research was
489 partially funded by EIPHI Graduate School (Contract 'ANR-17-EURE-0002').

490

491 **CRediT authorship contribution statement**

492 Nicolas Martin: Supervision; Writing – review & editing. Jean-Marc Cote: Data curation;
493 Software. Joseph Gavoille: Data curation; Validation. Jean-Yves Rauch: Validation;
494 Visualization.

495 All authors have read and agreed to the published version of the manuscript.

496

497 **References**

498 [1] J.P.B. Silva, K.C. Sekhar, H. Pan, J.L. MacManus-Driscoll, M. Pereira, Advances in
499 dielectric thin films for energy storage applications, revealing the promise of group IV binary
500 oxides, ACS Energy Lett. 6 (2021) 2208-2217. https://doi.org/10.1021/acsenergylett.1c00313

95

501 [2] U. Jansson, E. Lewin, Sputter deposition of transition -metal carbide thin films – A critical
502 review from a chemical perspective. Thin Solid Films. 536 (2013) 1-24.
503 https://doi.org/10.1016/j.tsf.2013.02.019
504 [3] Y.M. Kim, B.J. Lee, Modified embedded-atom method interatomic potentials for the Ti-C
505 and Ti-N binary systems. Acta Mater. 56 (2008) 3481-3489.
506 https://doi.org/10.1016/j.actamat.2008.03.027
507 [4] M. Magnusson, L. Hultmann, H. Högberg, Review of transition-metal diboride thin films.
508 Vacuum. 196 (2022) 110567-34. https://doi.org/10.1016/j.vacuum.2021.110567
509 [5] O. Wilhelmsson, J.P. Palmquist, E. Lewin, J. Emmerlich, P. Eklund, P.O.A. Persson, H.
510 Högberg, S. Li, R. Ahuja, O. Eriksson, L. Hultman, U. Jansson, Deposition and
511 characterization of ternary thin films within the Ti-Al-C system DC magnetron sputtering. J.
512 Cryst. Growth. 291 (2006) 290-300. https://doi.org/10.1016/j.jcrysgro.2006.03.008
513 [6] E. Lewin, D. Loch, A. Montagne, A.P. Ehiasarian, J. Patscheider, Comparison of Al-Si-N
514 nanocomposite coatings deposited by HIPIMS and DC magnetron sputtering. Surf. Coat.
515 Technol. 232 (2013) 680-689. https://doi.org/10.1016/j.surfcoat.2013.06.076
516 [7] J.F. Pierson, E. Tomasella, P. Bauer, Reactively sputtered Ti-B-N nanocomposite films:
517 Correlation between structure and optical properties. Thin Solid Films 408 (2002) 26-32.
518 https://doi.org/10.1016/s0040-6090(02)00071-8
519 [8] T. Minami, Transparent conducting oxide semiconductors for transparent electrodes.
520 Semicond. Sci. Tech. 20 (2005) S35-S44. https://doi.org/10.1016/b978-0-12-396489-2.00005-
521 9

522 [9] J. Lee, H. Seul, J.K. Jeong, Solution-processed ternary alloy aluminum yttrium oxide
523 dielectric for high performance indium zinc oxide thin-film transistors. J. Alloy. Compd. 741
524 (2018) 1021-1029. https://doi.org/10.1016/j.jallcom.2018.01.249
525 [10] C. Sandu, R. Sanjinès, F. Lévy, Formation of ternary nitride thin films by magnetron
526 sputtering co-deposition. Surf. Coat. Technol. 201 (2006) 4083-4089.
527 https://doi.org/10.1016/j.surfcoat.2006.08.100
528 [11] G. Abadias, L.E. Koutsokeras, S.N. Dub, G.N. Tolmachova, T. Debelle, T. Sauvage, P.
529 Villechaise, Reactive magnetron cosputtering of hard and conductive ternary nitride thin films:
530 Ti-Zr-N and Ti-Ta-N. J. Vac. Sci. technol. A28 (2010) 541-551.
531 https://doi.org/10.1116/1.3426296
532 [12] M.H. Tuilier, M.J. Pac, G. Covarel, C. Rousselot, L. Khoufach, Structural investigation
533 of thin films of $Ti_{1-x}Al_xN$ ternary nitrides using Ti K-edge X-ray absorption fine structure.
534 Surf. Coat. Technol. 201 (2007) 4536-4541. https://doi.org/10.1016/j.surfcoat.2006.09.095
535 [13] C. Woelfel, D. Bockhorn, P. Awakowicz, J. Lunze, Model approximation and
536 stabilization of reactive sputter processes, J. Process Control, 83 (2019) 121-128.
537 https://doi.org/10.1016/j.jprocont.2018.06.009
538 [14] F. Vaz, P. Cerqueira, L. Rebouta, S.M.C. Nascimento, E. Alves, P. Goudeau, J.P.
539 Rivière, K. Pischow, J. de Rijk, Structural, optical and mechanical properties of coloured
540 TiN_xO_y thin films. Thin Solid Films 447 (2004) 449-454. https://doi.org/10.1016/s0040-
541 6090(03)01123-4

101

542 [15] H. Barankova, S. Berg, P. Carlsson, C. Nender, Hysteresis effects in the sputtering
543 process using 2 reactive gases. Thin Solid Films 260 (1995) 181-186.
544 https://doi.org/10.1016/0040-6090(94)06501-2
545 [16] N. Martin, C. Rousselot, Instabilities of the reactive sputtering process involving one
546 metallic target and two reactive gases. J. Vac. Sci. Technol. A17(5) (1999) 2869-2878.
547 https://doi.org/10.1116/1.581953
548 [17] N. Martin, O. Banakh, A.M.E. Santo, S. Springer, R. Sanjinès, J. Takadoum, F. Lévy,
549 Correlation between processing and properties of TiO_xN_y thin films sputter deposited by the
550 reactive gas pulsing technique. Appl. Surf. Sci. 185 (2001) 123-133.
551 https://doi.org/10.1016/s0169-4332(01)00774-7
552 [18] A. Zairi, C. Nouveau, A.B.C. Larbi, A. Iost, N. Martin, A. Besnard, Effect of RGPP
553 process on properties of Cr-Si-N coatings. Surf. Eng. 30 (2014) 606-611.
554 https://doi.org/10.1179/1743294414y.0000000280
555 [19] N. Martin, J. Lintymer, J. Gavoille, J. Takadoum, Nitrogen gas pulsing to modify
556 properties of TiN_x thin films sputter deposited. J. Mater Sci. 37 (2002) 4327-4332.
557 https://doi.org/10.1023/A:1020600502303
558 [20] N. Martin, R. Sanjinès, J. Takadoum, F. Lévy, Enhanced sputtering of titanium oxide,
559 nitride and oxynitride thin films by the reactive gas pulsing technique. Surf. Coat. Technol.
560 142-144 (2001) 615-620. https://doi.org/10.1016/s0257-8972(01)01149-5
561 [21] M. Grafouté, K. Petitjean, A. Diama, J.F. Pierson, J.M. Greneche, C. Rousselot,
562 Structural investigations of iron oxynitride multilayered films obtained by the reactive gas

563 pulsing process. Surf. Coat. Technol. 272 (2015) 158-164.
564 https://doi.org/10.1016/j.surfcoat.2015.04.010
565 [22] A. Farhaoui, A. Bousquet, R. Smaali, A. Moreau, E. Centeno, J. Cellier, C. Bernard, R.
566 Rapegno, F. Reveret, E. Tomasella, Reactive gas pulsing process, a promising technique to
567 elaborate silicon oxynitride multilayer nanometric antireflective coatings. J. Phys. D: Appl.
568 Phys. 50 (2016) 015306-9. https://doi.org/10.1088/1361-6463/50/1/015306
569 [23] N. Martin, J. Lintymer, J. Gavoille, J.M. Chappé, F. Sthal, J. Takadoum, F. Vaz, L.
570 Rebouta, Reactive sputtering of TiO_xN_y coatings by the reactive gas pulsing process – Part I :
571 Pattern and period of pulses. Surf. Coat. Technol. 201 (2007) 7720-7726.
572 https://doi.org/10.1016/j.surfcoat.2007.03.002
573 [24] M. Fenker, H. Kappl, C.S. Sandu, Precise control of multilayered structures of Nb-O-N
574 thin films by the use of reactive gas pulsing process in DC magnetron sputtering. Surf. Coat.
575 Technol. 202 (2008) 2358-2362. https://doi.org/10.1016/j.surfcoat.2007.08.007
576 [25] H. Le Dreo, O. Banakh, H. Keppner, P.A. Steinmann, D. Brian, N.F. de Rooij, Optical,
577 electrical and mechanical properties of the tantalum oxynitride thin films deposited by pulsing
578 reactive gas sputtering. Thin Solid Films 515 (2006) 952-956.
579 https://doi.org/10.1016/j.tsf.2006.07.054
580 [26] J.M. Chappé, P. Carvalho, S. Lanceros-Mendez, M.I. Vasilevskiy, F. Vaz, A.V.
581 Machado, M. Fenker, H. Kappl, N.M.G. Parreira, A. Cavaleiro, Influence of air oxidation on
582 the properties of decorative NbO_xN_y coatings prepared by gas pulsing. Surf. Coat. Technol.
583 202 (2008) 2363-2367. https://doi.org/10.1016/j.surfcoat.2007.09.015

107

584 [27] P. Carvalho, L. Cunha, E. Alvez, N. Martin, E. Le Bourhis, F. Vaz, ZrO_xN_y decorative
585 thin films prepared by the reactive gas pulsing process. J. Phys. D: Appl. Phys. 42 (2009)
586 195501-7. https://doi.org/10.1088/0022-3727/42/19/195501

587 [28] K. Petitjean, M. Grafouté, C. Rousselot, J.F. Pierson, Reactive gas pulsing process: A
588 method to extend the composition range in sputtered iron oxynitride films. Surf. Coat.
589 Technol. 202 (2008) 4825-4829. https://doi.org/10.1016/j.surfcoat.2008.04.064

590 [29] N. Martin, J. Lintymer, J. Gavoille, J.M. Chappé, F. Sthal, J. Takadoum, F. Vaz, L.
591 Rebouta, Reactive sputtering of TiO_xN_y coatings by the reactive gas pulsing process – Part II :
592 The role of the duty cycle. Surf. Coat. Technol. 201 (2007) 7727-7732.
593 https://doi.org/10.1016/j.surfcoat.2007.03.021

594 [30] N. Martin, C. Rousselot, Modelling of reactive sputtering involving two separated
595 metallic targets. Surf. Coat. Technol. 114 (1999) 235-249. https://doi.org/10.1016/s0257-
596 8972(99)00051-1

597 [31] S. Berg, E. Särhammar, T. Nyberg, Upgrading the "Berg-model" for reactive
598 sputtering processes. Thin Solid Films 565 (2014) 186-192.
599 https://doi.org/10.1016/j.tsf.2014.02.063

600 [32] D. Depla, R. De Gryse, Target poisoning during reactive magnetron sputtering: Part I:
601 The influence of ion implantation. Surf. Coat. Technol. 183 (2004) 184-189.
602 https://doi.org/10.1016/j.surfcoat.2003.10.006

110

603 [33] D. Depla, Z.Y. Chen, A. Bogaerts, V. Ignatova, R. De Gryse, R. Gijbels, Modeling of
604 the target surface modification by reactive ion implantation during magnetron sputtering. J.
605 Vac. Sci. Technol. A22 (2004) 1524-1529. https://doi.org/10.1016/j.surfcoat.2003.10.006
606 [34] N. Martin, A. Besnard, F. Sthal, J. Takadoum, The reactive gas pulsing process for
607 tuneable properties of sputter deposited titanium oxide, nitride and oxynitride coatings. Inter.
608 J. Mater. Prod. Technol. 39 (2010) 159-177. https://doi.org/10.1504/ijmpt.2010.034268

Figure captions

Figure 1

Oxygen and nitrogen mass flow rates as a function of the time implemented during the sputter-deposition of Ti-O-N thin films. A rectangular signal is used for both reactive gases, which are independently and periodically pulsed during the deposition. All pulsing parameters can be tuned for each gas. T_{O2} *= pulsing period of* O_2 *(s),* T_{N2} *= pulsing period of* O_2 *(s),* δ *= delay time between the starting point of* N_2 *and* O_2 *pulsing (s),* q^{O2}_{min} *= minimum* O_2 *flow rate (sccm),* q^{N2}_{min} *= minimum* N_2 *flow rate (sccm),* q^{O2}_{Max} *= maximum* O_2 *flow rate (sccm),* q^{N2}_{Max} *= maximum* N_2 *flow rate (sccm),* t^{O2}_{ON} *= time of* O_2 *injection at* q^{O2}_{Max} *(s),* t^{O2}_{OFF} *= time of* O_2 *injection at* q^{O2}_{min} *(s),* t^{N2}_{ON} *= time of* N_2 *injection at* q^{N2}_{Max} *(s),* t^{N2}_{OFF} *= time of* N_2 *injection at* q^{N2}_{min} *(s).*

Figure 2

Ti-O-N deposition rate as a function of the oxygen duty cycle α_{O2} *and for various nitrogen duty cycles* α_{N2}*. Both reactive gases are pulsed with the same period, i.e.,* $T = T_{O2} = T_{N2} = 45$ *s, and the delay time* $\delta = 34$ *s (i.e., 75% of the pulsing period T). Ti, TiN and* TiO_2 *deposition rates are also specified in pure argon atmosphere, when nitrogen and oxygen are constantly injected at* q_{N2Max} *and* q_{O2Max}*, respectively. Operating conditions noted "A" and "B" will be discussed from real time measurements of Ti target potential and total sputtering pressure.*

Figure 3

116

630 *a) Optical transmittance at 633 nm and b) DC electrical conductivity at room temperature vs.*

631 *oxygen duty cycle of Ti-O-N thin films 400 nm thick deposited on glass substrates for various*

632 *nitrogen duty cycles. A smooth transition can be obtained from absorbent Ti-O-N films*

633 *colored in the bulk, to interferential* TiO_2*-like compounds as a function of oxygen and*

634 *nitrogen duty cycles. It also correlates with a significant change of the electrical properties*

635 *from conducting to semi-conducting and finally insulating behaviors. Optical and electrical*

636 *properties of films prepared following "A" and "B" points (as reported in Fig. 2) are also*

637 *given.*

638

639 Figure 4

640 *a) Real time measurements of Ti target potential and total sputtering pressure recorded*

641 *during Ti-O-N film deposition setting* α_{N2} = 80% *of* T_{N2} *and* α_{O2} = 22% T_{O2}. *Pulsing period T =*

642 $T_{O2} = T_{N2}$ = 45 *s and delay time* δ = 34 *s. These operating conditions correspond to the*

643 *preparation of semi-absorbent films (point "A" in Fig. 2 and 3). b) Real mass flow rates vs.*

644 *time of oxygen and nitrogen gases are also specified and can be easily compared to response*

645 *times of potential and pressure.*

646

647 Figure 5

648 *a) Real time measurements of Ti target potential and total sputtering pressure recorded*

649 *during Ti-O-N film deposition setting* α_{N2} = 25% *of* T_{N2} *and* α_{O2} = 22% T_{O2}. *Pulsing period T =*

650 $T_{O2} = T_{N2}$ = 45 *s and delay time* δ = 34 *s. These operating conditions correspond to the*

119

651 *preparation of absorbent films (point "B" in Fig. 2 and 3). b) Real mass flow rates vs. time of*

652 *oxygen and nitrogen gases are also specified and can be easily compared to response times of*

653 *potential and pressure.*

654

655 Figure 6

656 *a) Real time measurements of Ti target potential and total sputtering pressure recorded*

657 *during Ti-O-N film deposition for various* α_{N2} *and* α_{O2} *duty cycles. Pulsing period* $T = T_{O2} =$

658 $T_{N2} = 45$ *s and delay time* $\delta = 34$ *s. Real mass flow rates (RMF) vs. time for oxygen and*

659 *nitrogen gases are also shown.*

660

661 Figure 7

662 *2D qualitative diagram for the reactive sputtering of Ti-O-N thin films by RGPP with an*

663 *independent pulsing of oxygen and nitrogen reactive gases. Occurrence of different reactive*

664 *sputtering modes (elemental, nitrided or oxidized) are defined as a function of* O_2 *and* N_2 *duty*

665 *cycles. A periodic alternation of the process between 2 or 3 modes can be tuned by means of*

666 *an accurate control of both duty cycles. Points "A" and "B" are also indicated from*

667 *operating conditions defined in Fig. 2.*

668

669 Figure 8

670 *Fig. 8. Ternary phase diagram illustrating the range of chemical compositions which can be*

671 *achieved in titanium oxynitride thin films sputter-deposited pulsing only* O_2 *gas and keeping*

122

672 *constant N_2 flow rate(red circles from [34]), or pulsing independently both reactive gases*
673 *(region defined by the dotted black line with points "A" and "B" - black squares - as defined*
674 *previously from Fig. 2). Compositions of TiN_x and TiO_x films produced by RGPP introducing*
675 *and pulsing only one reactive gas (N_2 and O_2, respectively) are also indicated (green and blue*
676 *circles, respectively).*